Experimental Neurology 239 (2013) 28–37

Contents lists available at SciVerse ScienceDirect

Experimental Neurology

journal homepage: www.elsevier.com/locate/yexnr

Environmental enrichment prevents astroglial pathological changes in the hippocampus of APP transgenic mice, model of Alzheimer's disease

Juan Beauquis [a,b], Patricio Pavía [a], Carlos Pomilio [a], Angeles Vinuesa [a], Natalia Podlutskaya [c,d], Verónica Galvan [c,d], Flavia Saravia [a,b,*]

[a] Laboratorio de Neurobiología, Departamento de Química Biológica, Facultad de Ciencias Exactas y Naturales, Universidad de Buenos Aires, Argentina
[b] Instituto de Biología y Medicina Experimental, CONICET, Buenos Aires, Argentina
[c] Department of Physiology, University of Texas Health Science Center at San Antonio, Texas, USA
[d] The Barshop Institute for Longevity and Aging Studies, University of Texas Health Science Center at San Antonio, Texas, USA

ARTICLE INFO

Article history:
Received 24 July 2012
Revised 4 September 2012
Accepted 20 September 2012
Available online 28 September 2012

Keywords:
Astrocytes
Hippocampus
Transgenic mice
Alzheimer's disease
Environmental enrichment
GFAP

ABSTRACT

Alzheimer's disease (AD) is a neurodegenerative disease that affects neurons and glial cells and leads to dementia. Growing evidence shows that glial changes may precede neuronal alterations and behavioral impairment in the progression of the disease. The modulation of these changes could be addressed as a potential therapeutic strategy. Environmental enrichment has been classically associated to effects on neuronal morphology and function but less attention has been paid to the modulation of glia. We thus characterized astroglial changes in the hippocampus of adult PDAPP-J20 transgenic mice, a model of AD, exposed for 3 months to an enriched environment, from 5 to 8 months of age. Using confocal microscopy, three-dimensional reconstruction and Sholl analysis, we evaluated the morphology of two distinct populations of astrocytes: those associated to amyloid β plaques and those that were not. We found that plaque-associated astrocytes in PDAPP-J20 mice had an increased volume and process ramification than control astrocytes. Non-plaque-associated astrocytes showed a decrease in volume and an increase in the ramification of GFAP+ processes as compared with control astrocytes. Environmental enrichment prevented these alterations and promoted a cellular morphology similar to that found in control mice. Morphological changes in non-plaque-associated astrocytes were found also at 5 months of age, before amyloid β deposition in the hippocampus. These results suggest that glial alterations have an early onset in AD pathogenesis and that the exposure to an enriched environment is an appropriate strategy to reverse them. Cellular and molecular pathways involved in this regulation could constitute potential novel therapeutic targets.

Introduction

Alzheimer's disease (AD) is an age-related neurodegenerative disorder and the most common cause of dementia among older people. The fundamental signs include language alterations, memory loss and progressive cognitive impairment (Mayeux, 2010; Querfurth and LaFerla, 2010). Patients suffering from AD show atrophic changes in brain regions involved in learning and memory, as a result of synaptic degeneration and neuronal death (Mattson, 2004). Extracellular neuritic plaques of misfolded amyloid β peptides and intracellular neurofibrillary tangles composed of hyperphosphorylated tau protein are the major histopathological hallmarks of AD (Mattson, 2004; Braak and Braak, 1998; Dickson, 1997). Soluble amyloid β peptides are generated after the sequential cleavage of the amyloid precursor protein (APP), and can undergo oligomerization, aggregate into fibrils and form amyloid plaques. The Aβ 1–42 peptide is considered the most toxic species and a correlation between the levels of soluble Aβ peptides and the degree of synaptic loss and cognitive impairment has been described (Lue et al., 1999). However, the pathophysiology of AD is far from being understood and, in spite of extensive biomedical scientific efforts, the currently available treatments only offer a partial and transient improvement of symptoms and a mild delay in the progression of the disease (Massoud and Leger, 2011).

There is a growing body of evidence suggesting that amyloid plaques and neurofibrillary tangles are not the first pathological changes in AD. Remarkably, the glial involvement in the pathogenesis of AD was originally suggested by Alois Alzheimer when he demonstrated that the neuritic plaque included glial cells (Heneka et al., 2010). Later, the close association between astroglia and brain pathology was recognized in a wide range of conditions, including AD, cerebral ischemia and epilepsy among others (Nagele et al., 2004; Nedergaard and Dirnagl, 2005; Tian et al., 2005; Giaume et al., 2007). Both acute and chronic brain damage are accompanied by a specific morpho-functional remodeling of astrocytes that tend

* Corresponding author at: Instituto de Biología y Medicina Experimental, Vuelta de Obligado 2490, Buenos Aires 1428, Argentina.
E-mail address: fesaravia@gmail.com (F. Saravia).

0014-4886/$ – see front matter © 2012 Elsevier Inc. All rights reserved.
http://dx.doi.org/10.1016/j.expneurol.2012.09.009

to isolate the damaged area, rebuild the blood–brain barrier and facilitate the adaptation of brain circuits in damaged areas, a process known as astrogliosis (Pekny and Nilsson, 2005).

Astrogliosis is a universal feature of AD brains and of transgenic mice modeling the disease. Reactive GFAP+ astrocytes surround amyloid plaques and participate in neuritic plaque formation as well as in a local inflammatory response (Nagele et al., 2004; Heneka et al., 2010; Rodriguez et al., 2009). A number of reports demonstrated that astrocytes can accumulate substantial amounts of Aβ 1–42 intracellularly (Akiyama et al., 1999; Nagele et al., 2004; Thal et al., 2000). Complementary, *in vitro* studies showed that astrocytes can be activated by Aβ 1–42 oligomers and secrete inflammatory molecules such as IL-1β (Hou et al., 2011). This evidence strongly suggests a key role of astrocytes in the modulation of amyloid β-induced cell toxicity in the brain.

In the particular context of neurodegeneration, astrocytes can progressively lose their neuroprotective functions associated to energy metabolism (Li et al., 1997), glutamate recycling (Masliah et al., 1996) and glutathione supply (Fuller et al., 2010; Newman et al., 2007; Steele and Robinson, 2012). Some studies have suggested that glial dysfunction may be an early event in the neurodegenerative process (Rodriguez et al., 2009). In one study, Yeh et al. reported premature glial atrophy in hippocampus and entorhinal cortex of the triple transgenic (3xTg-AD) AD model before plaque deposition, in association with changes in the expression of inflammatory mediators (Yeh et al., 2011). Astroglial ERK activation and astrogliosis were described in mid-frontal cortex of post-mortem samples from early AD patients (Webster et al., 2006). Another study found that patients with mild cognitive impairment present astrogliosis in cortical and subcortical regions, evidenced by PET scanning, suggesting it as an early phenomenon in the development of AD (Carter et al., 2012).

Environmental enrichment (EE) provides physical activity, learning experiences, increased somatosensorial and visual inputs and social interaction (van Praag et al., 2000; Hebb, 1947; Krech et al., 1962) and, in rodents, it is able to increase neuro- and gliogenesis, enhance cognition, and to promote the recovery from brain injury and/or neurodegeneration in association with changes in lymphocyte functional activities and cytokine and interleukin profile (Beauquis et al., 2010; Bindu et al., 2007; Kempermann et al., 1997; Kempermann et al., 1998; Nithianantharajah and Hannan, 2006; Arranz et al., 2011). Interestingly, astrocytes could also be able to react to environmental stimuli, jointly with neurons (Sirevaag and Greenough, 1991; Viola et al., 2009). The environment plays a fundamental role in neurodegenerative and psychiatric diseases, though the effect of EE in AD models is a matter of controversy. Environmental enrichment was associated with increased adult hippocampal neurogenesis in APP23 mice (Mirochnic et al., 2009) and also improved learning and memory in APP_{swInd} mice (Valero et al., 2011). However, EE had no effect on these parameters in APP/PS1K1 mice (Cotel et al., 2012). The cognitive reserve hypothesis explains that previous brain activity associated to educational duration and attainment may allow the brain to cope with the pathology by neural and reserve compensation (Murray et al., 2011).

While EE in animal models and a high educational level in humans are known to be implicated in the improvement of cognitive reserve and neuronal plasticity, thus delaying the onset of clinical symptoms in different neurodegenerative diseases, these strategies are probably also associated with the modulation of degenerative changes and amyloid pathology through multiple pathways (Briones et al., 2009; Costa et al., 2007; Herring et al., 2008; Lazarov et al., 2005).

To our knowledge, this is the first study to assess the influence of EE on astroglial morphology in an animal model of AD. Given its potential significance for neural protection, we hypothesized that EE may modulate the glial phenotype in hippocampus of transgenic PDAPP-J20 mice, a well established model of AD. To this aim, we studied morphological changes of GFAP+ astrocytes in the stratum radiatum of 5 and 8 month-old transgenic and non transgenic PDAPP-J20 mice before and after exposure to an enriched environment.

Materials and methods

Animals

The derivation and characterization of PDAPP-J20 [hAPP(J20)] mice have been described elsewhere (Galvan et al., 2006; Hsia et al., 1999; Mucke et al., 2000; Roberson et al., 2007; Selkoe, 2000). PDAPP-J20 mice carrying the Swedish and Indiana APP human mutations were maintained by heterozygous crosses with C57BL/6J mice (Jackson Laboratories, Bar Harbor, ME) in our animal facility (Institute of Biology and Experimental Medicine, UBA–CONICET; NIH Assurance Certificate # A5072-01) and were housed under controlled conditions of temperature (22 °C) and humidity (50%) with 12 h/12 h light/dark cycles (lights on at 7:00 am). PDAPP-J20 mice were heterozygous with respect to the transgene, verified by RT PCR using specific primers. All animal experiments followed the NIH Guide for the Care and Use of Laboratory Animals and were approved by the Ethical Committee of the Institute of Biology and Experimental Medicine. All efforts were done to reduce the number of mice used in the study as well as to minimize animal suffering and discomfort.

Female transgenic mice (Tg) and their non-transgenic siblings (NTg) were housed in an enriched environment (EE) or in standard conditions (SC) during 3 months (5 to 8 months of life, n = 5 per group). Additionally, a group of 5 month-old Tg and NTg mice (n = 5 per group) housed in SC was analyzed separately to evaluate brain changes at a time-point matching the starting age of animals under the EE protocol (Fig. 1). In both SC and EE conditions, water and regular rodent chow were available *ad libitum* and the floor was covered with 2 cm of wooden chips. The dimensions of standard cages were X = 17.5 cm, Y = 27.5 cm, (481.25 cm^2) and Z = 15 cm (height) with 2–3 mice per cage. The enriched environment consisted of larger cages measuring X = 40 cm, Y = 33 cm (1320 cm^2) and Z = 15 cm with 5 mice per cage. Toys, extra nesting material, small plastic houses and tubes were available in the enriched condition (Fig. 1), with a rearrangement of elements every 2 days. Running wheels were not provided. At the end of the experiment, animals were anesthetized with ketamine (80 mg/kg BW, i.p.; Holliday-Scott, Argentina) and xylazine (10 mg/kg BW, i.p.; Bayer, Argentina) and then transcardially perfused with 30 mL of 0.9% saline followed by 30 mL of 4% paraformaldehyde in 0.1 M phosphate buffer, pH 7.4. Brains were removed from the skull, dissected, fixed overnight in the 4% paraformaldehyde solution at 4 °C and then cut coronally at 60 μm in a vibrating microtome (Vibratome 1000P). Sections were stored in a cryoprotectant solution (25% glycerol, 25% ethylene glycol, 50% phosphate buffer 0.1 M, pH 7.4) at −20 °C until use. All immunohistochemical techniques and Congo red staining were performed on free-floating sections.

Human Aβ 1–40 and Aβ 1–42 peptides in brain homogenates

Another experiment was carried out (n = 4 mice per group) to measure amyloid beta peptides (Aβ). Human Aβ 1–40 and Aβ 1–42 peptide levels were measured in guanidine hemi-brain homogenates using specific sandwich ELISA assays (Invitrogen, USA) as previously described (Galvan et al., 2006; Spilman et al., 2010) and following the manufacturer's instructions. Briefly, the wet mass of each mouse hemibrain was determined, and cold 5 M guanidine HCl/50 mM Tris HCl was added (final concentration: 100 mg/mL), thoroughly homogenized, sonicated and followed by gentle shaking during 6 h at room temperature (RT). Then, the samples were diluted with cold reaction buffer (1:50; Dulbecco's phosphate buffered saline with 5% BSA and 0.03% Tween-20) supplemented with 1× Protease Inhibitor Cocktail (Calbiochem, USA) and centrifuged at 16,000×*g* for 20 min at 4 °C. The supernatants were stored on ice. Amyloid β 1–40 and 1–42 peptides were separately measured. Fifty microliters of standards corresponding to calibration curve or samples were added to the wells preabsorbed with specific antibody against Aβ 1–40 or 1–42 made

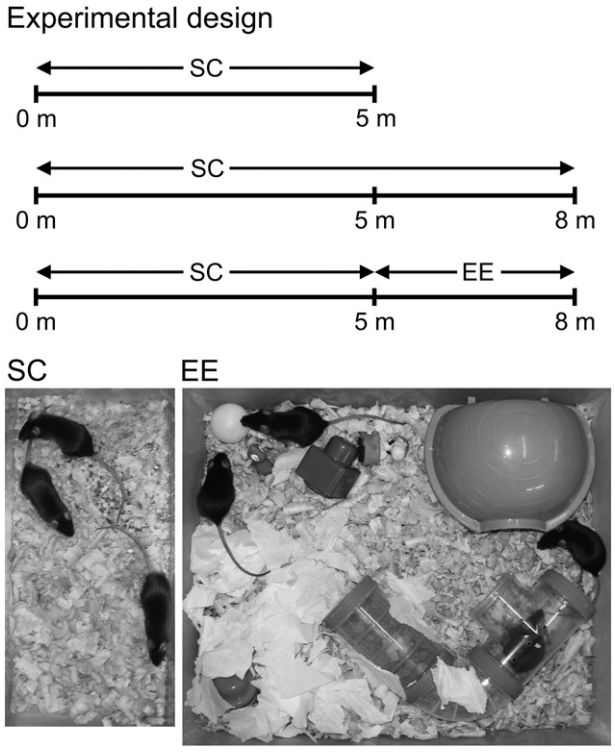

Fig. 1. Experimental protocol. Transgenic and non-transgenic female PDAPP-J20 mice were evaluated following three different experimental designs. A group of mice was studied at 5 months of age (5 m), after housing in standard conditions (SC) since birth (top timeline). The other 2 groups were studied at 8 months of age (8 m). One group was housed in SC since birth (middle timeline) and the other was housed in SC from birth to 5 m and in an enriched environment (EE) from 5 m to 8 m (bottom timeline). The photographs at the bottom represent the 2 caging conditions. The SC consisted in rearing mice in standard animal facility cages with 2 or 3 animals per cage. The EE consisted in housing animals in cages of larger size, with toys, additional nesting material, tunnels and shelters in groups of 5 mice per cage. The arrangement of elements in the EE was changed 3 times per week and some objects were replaced by novel ones.

in rabbit. The following step included the addition of another specific antibody developed in rabbit and incubation during 3 h. After aspiration and washes, an incubation with HRP anti-rabbit antibody was performed for 30 min at RT. After washes and exposure to a stabilized chromogen, the reaction was stopped and absorbance of standards and samples was read at 450 nm. The performance characteristics of the ELISA assays including precision, linearity of dilution, recovery and antigenic specificity were determined and informed by the manufacturer. The minimum detectable amount of human Aβ 1–40 was 6 pg/mL; while for Aβ 1–42 was 13 pg/mL.

Congo red staining

The number and size of amyloid plaques in strata radiatum and lacunosum-moleculare, corresponding to the CA1 subfield, were assessed in brain sections stained with Congo red (protocol available in Wilcock et al., 2006). Briefly, coronal brain sections were incubated for 5 min at room temperature (RT) in a solution containing 0.2% Congo red (Biopack, Argentina), 3% NaCl (to saturation) and 0.01% sodium hydroxide in 80% ethanol. After rinsing, sections were put on gelatin-coated slides, air-dried overnight, dehydrated using ethanol and cleared in xylene. Slides were coverslipped using Canada balsam (Biopack, Argentina).

Analysis of sections stained with Congo red

Specific staining of amyloid deposits with Congo red was confirmed by performing an immunohistochemistry for amyloid β in parallel sections from the same animals, yielding similar plaque counts. Congo red-stained sections were preferred to quantify plaque density and area as they provided a higher specific signal/background ratio than immunohistochemistry. The protocol used for amyloid β immunohistochemistry is described in the following section. Images from Congo red stained sections were obtained under a 40× magnification in a Nikon Eclipse E200 microscope. The number of plaques and their area were measured using the Optimas 6.5 software (Media Cybernetics). On each section, an area including strata radiatum and lacunosum-moleculare under CA1 of the dorsal hippocampus was delimited. Using an appropriate user-defined threshold, red stained amyloid plaques were identified in number and size inside this region of interest. Total number of plaques in the CA1 region was estimated using Cavalieri principle ($V = T \times \sum A$). Plaque load was expressed as the percent of CA1 area covered by Aβ plaques.

Immunohistochemistry

Immunohistochemistry was done to determine number, volume and morphology of GFAP+ cells. Double immunohistochemistry for GFAP and amyloid β allowed us to evaluate the association of GFAP+ astrocytes with amyloid β deposits. Additionally, NeuN immunohistochemistry was done to estimate the volume of the analyzed hippocampal regions. For the double GFAP/amyloid β immunohistochemistry, antigen retrieval was achieved by heating sections in 0.01 M citrate buffer in a thermostatic bath at 85 °C. After blocking with 2% non-fat milk, sections were incubated overnight at 4 °C with the following primary antibodies: rabbit polyclonal anti-GFAP (1:300, G-9269, Sigma) and mouse monoclonal anti-amyloid β (1:700, 4G8, MAB 1561, Chemicon). After incubation with secondary fluorescent antibodies (anti-rabbit Alexa 488 and anti-mouse Alexa 555, Invitrogen), sections were put on gelatin-coated slides and mounted with Fluoromount G (SouthernBiotech, USA). For NeuN immunohistochemistry, unspecific binding sites were blocked with 1% normal horse serum before the overnight incubation with mouse monoclonal anti-NeuN antibody (1:250, MAB 377, Chemicon, USA) at 4 °C. For detection we used a biotinylated anti-mouse secondary antibody (Vector Laboratories) followed by processing with the ABC kit (Vector Laboratories) and development with 2 mM diaminobenzidine (Sigma, USA) and 0.5 mM H_2O_2 in 0.1 M Tris buffer at RT. Sections were put on gelatin-coated slides, air-dried overnight, dehydrated in graded solutions of ethanol, cleared in xylene and mounted with Canada balsam.

Analysis of GFAP+ cells

The number of GFAP immunopositive cells was assessed in the CA1 hippocampal subfield, using a modified version of the optical disector method (Gundersen et al., 1988). Images were obtained from anatomically matched areas from coronal brain sections, representative of the whole extension of the dorsal hippocampus, using a Nikon Eclipse E80 confocal microscope with a 40× air objective. Serial confocal images were obtained along the Z axis (0.65 μm step) of each analyzed section to make a three-dimensional reconstruction of the tissue using NIH software ImageJ (Abramoff et al., 2004). The density of GFAP+ cells (number of cells/unit of volume) was quantified using a randomly-placed 0.0024 mm^3 counting probe. A minimum of 100 cells was counted per animal. For the calculation of the total number of cells, the volume of the studied regions was estimated using the Cavalieri principle ($V = T \times \sum A$) on serial sections processed for NeuN immunohistochemistry. Areas (A) were measured using Optimas image analysis software (Media Cybernetics) and the T value was obtained by multiplying the number of sections and the distance between planes.

Volume and morphology of GFAP+ cells were evaluated in 2 different cell populations: those cells that were located near amyloid plaques (plaque-associated cells) and those that were far from

plaques (non-plaque-associated cells). Plaque-associated (PA) cells were those found in close apposition to amyloid plaques while non-plaque-associated (NPA) cells were those that were located at least at 50 μm from the edges of plaques.

The volume of individual GFAP+ cells was estimated on three-dimensional reconstructed images obtained from confocal Z-stacks using ImageJ software. Cells entirely located inside the analyzed sections, presenting a complete staining and not overlapping with other cells or blood vessels were considered for counting. A minimum of 25 cells evenly distributed across sections were analyzed per animal. A threshold was applied to images to exclude eventual unspecific staining. After the binarization of images, the cell volume was estimated using Cavalieri principle as described above. Results are presented in μm^3.

Sholl analysis of GFAP+ cells was done on averaged images of confocal Z-stacks following a previously published protocol (Beauquis et al., 2010). The criterion for the selection of cells was the same as for the volume estimation. Each cell was manually traced to obtain a binary image devoid of background staining. A minimum of 25 GFAP+ cells per animal were included in this analysis. Binarized images were scaled and analyzed with ImageJ running Sholl Analysis Plugin v1.0 (written by Tom Maddock and available at http://www-biology.ucsd.edu/labs/ghosh/software/index.html). Briefly, this technique (Sholl, 1953) consists in superimposing a grid with concentric rings or shells distributed at equal distances that are centered on the soma of the cell. The number of processes intersected per shell is computed and branching/shape complexity is evaluated. Results are presented as the mean number of intersections per each radius-defined circle.

Statistical analysis

Data are expressed as the mean ± SEM. Statistical analyses were performed using unpaired two-tailed Student's *t* test, one-way ANOVA, two-way ANOVA and RM ANOVA, as indicated in Results section. Bonferroni's *post hoc* test was applied after ANOVA. Variables considered were "genotype" (NTg or Tg mice) and "housing" (standard caging or enriched environment). Values of $p<0.05$ for differences between group means were significant. Analyses were done using Prism 3.02 software (GraphPad Software Inc.).

Results

Environmental enrichment is associated with diminished levels of Aβ 1–40 and 1–42 peptides in transgenic mice

To determine whether environmental enrichment affects the levels of Aβ 1–40 and 1–42 in PDAPP-J20 mouse brains, human Aβ 1–40 and 1–42 peptides were measured in brain homogenates by specific sandwich ELISA (Figs. 2A and B). In NTg mice these peptides were undetectable. In 5-month-old (5 m) Tg mice, low levels of both peptides were measured. Amyloid β 1–40 and 1–42 were significantly increased in Tg mice at 8 months (8 m; $p<0.05$ *vs.* NTg; one-way ANOVA, Bonferroni's *post hoc* test). After a 3-month exposure to EE, levels of both peptides were significantly decreased in Tg mice compared with Tg mice housed in standard caging (SC; $p<0.05$).

Number of amyloid plaques and plaque load in the hippocampus

To determine whether amyloid deposition would be affected by EE in PDAPP-J20 mice, number and area of Congo red-stained amyloid plaques were quantified (Figs. 2C, E, and F) in CA1 hippocampal region. Very few plaques were found in hippocampus of 5 m Tg mice maintained in SC (12.04 plaques per CA1 region of the hippocampus). In contrast, 173.2 ± 37.9 plaques were present in hippocampus of 8 m Tg mice. A trend to decreased numbers of Congo red-positive deposits was observed, however, in 8 m Tg mice exposed to EE (124 ± 19.98 plaques; $p=0.31$, unpaired two-tailed Student's *t* test). A similar trend was observed in the analysis of CA1 hippocampal plaque load ($p=0.24$ Tg SC *vs.* Tg EE). The reference areas were similar in all groups (Tg 5 m $1.38\pm0.2\times10^6$, Tg 8 m SC $1.37\pm0.4\times10^6$, Tg 8 m EE $1.03\pm0.15\times10^6$; mm^2). Complementary, an immunofluorescence study to specifically detect the amyloid β deposits (fragment 17–24) revealed and confirmed the presence of extracellular plaques in the hippocampus of Tg mice (representative image shown in Fig. 2D).

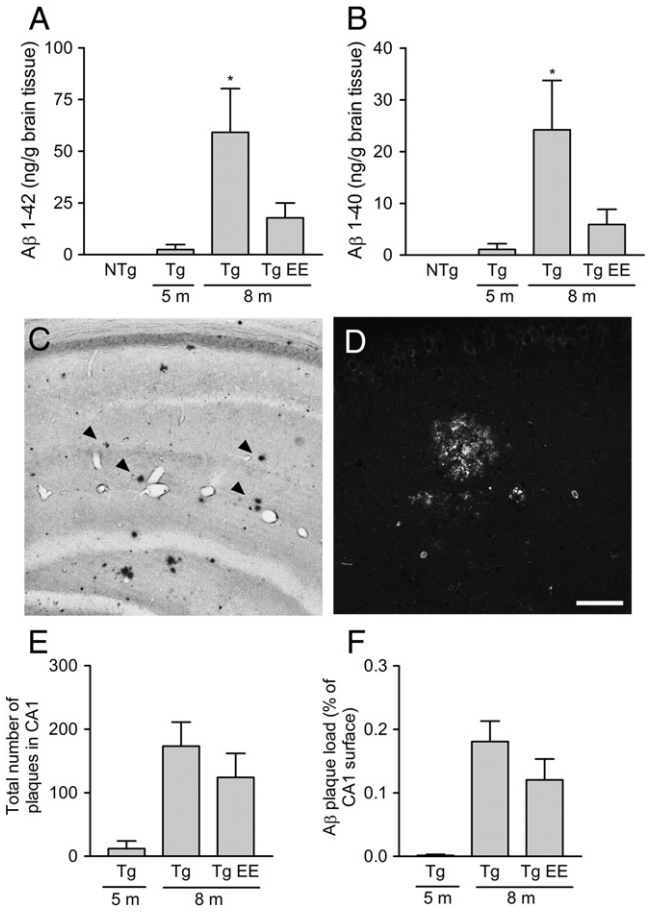

Fig. 2. Amyloid β (Aβ) content. Panels A and B show the levels of Aβ peptides 1–42 and 1–40 measured with ELISA in total brain homogenates. At 5 months (5 m), Tg mice showed low levels of both peptides while at 8 months (8 m) high levels were detected. The exposure of Tg mice to environmental enrichment (Tg EE) reduced the content of peptides (*$p<0.05$ Tg SC *vs.* NTg and Tg EE; one-way ANOVA, Bonferroni's *post hoc* test). Panel C shows a representative image of Congo red staining in the hippocampus of an 8 m old Tg mouse. Arrowheads point at amyloid plaques located in strata radiatum and lacunosum-moleculare. The scale bar represents 200 μm. Panel D shows a confocal image of an amyloid plaque detected by immunofluorescence. The scale bar represents 50 μm. Quantifications of total number of plaques (panel E) and Aβ plaque load (panel F), determined in CA1 region on Congo-red stained sections, are shown in panels E and F. Very few plaques were found in 5 m Tg mice. At 8 months, Tg mice presented numerous plaques while the exposure to an enriched environment did not have a significant effect.

Transient decreased number of hippocampal astrocytes at an early pathological stage in transgenic mice

To determine whether differences in astrocyte number in the hippocampus existed across genotype and housing conditions, astrocytic cell bodies and processes were identified in the hippocampus of PDAPP-J20 mice by expression of GFAP, a frequently used marker for astroglia (Fig. 3A). Astrocyte number was measured using stereological analyses of confocal Z-stacks. The number of GFAP+ cells in 5 m Tg mice was significantly reduced in comparison to that corresponding to age-matched NTg control animals ($p<0.01$ Tg *vs.* NTg, unpaired two-tailed Student's *t* test; Fig. 3B). At 8 m, a trend towards

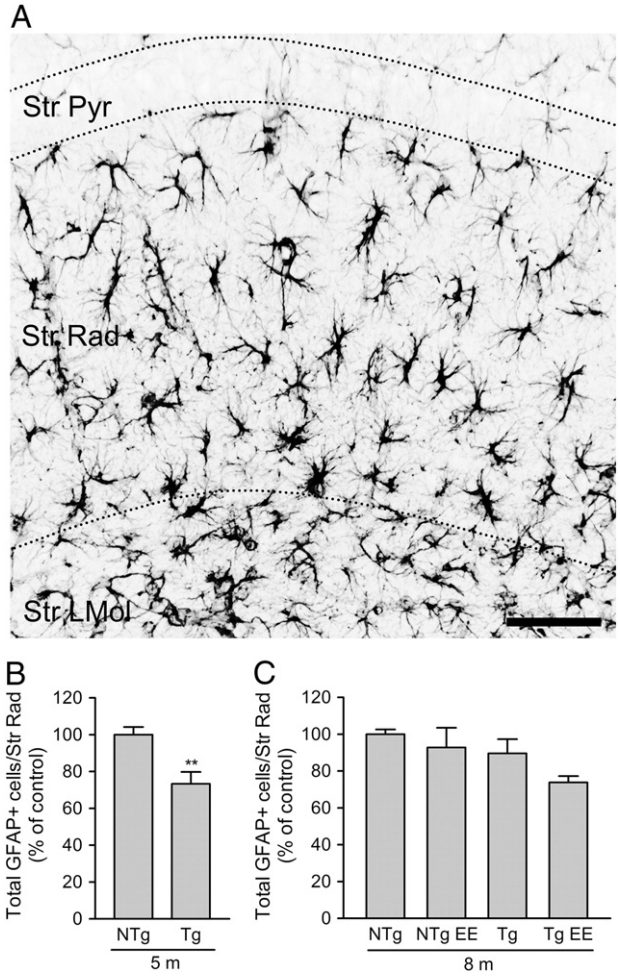

Fig. 3. Number of GFAP+ astrocytes in stratum radiatum of CA1 hippocampal region. Confocal images were obtained from the CA1 region in brain sections processed for GFAP immunohistochemistry. In panel A, an averaged and inverted image of multiple confocal planes is shown (Str Pyr, stratum pyramidale; Str Rad, stratum radiatum; Str LMol, stratum lacunosum-moleculare). Scale bar represents 50 μm. At 5 months of age (5 m), Tg animals showed a decrease in the number of GFAP+ astrocytes compared with NTg ($p<0.01$; unpaired two-tailed *t* test; panel B). At 8 months (8 m) no differences were found between the experimental groups (panel C). Results are expressed as the percentage of cells compared to the control group.

decreased numbers of GFAP+ cells in Tg animals was observed when comparing with NTg of the same age ($p=0.06$; two-way ANOVA). The reference volume of the stratum radiatum and lacunosum-moleculare was obtained from a set of sections processed in parallel and reacted with NeuN antibody as a marker for neurons. No significant differences were found between experimental groups at either age (5 m: NTg $21.36\pm0.74\times10^8$, Tg $19.67\pm0.18\times10^8$, $p=0.42$; 8 m: NTg $17.5\pm0.47\times10^8$, NTg EE $16.75\pm2.26\times10^8$, Tg $17.47\pm1.58\times10^8$, Tg EE $14.09\pm1.21\times10^8$, μm^3, $p=0.39$ for genotype, $p=0.20$ for housing; two-way ANOVA).

Volume changes in hippocampal astrocytes depend on the proximity to amyloid deposits. Effect of enriched environment

To determine whether astrocytic volume was modified by genotype and housing variables, we determined volumes of GFAP+ astrocytes in the CA1 hippocampal region using three-dimensional projections of confocal stack images (Fig. 4A). As shown in Fig. 4E, no differences in astrocytic volumes were observed in Tg as compared to NTg mice at 5 m ($p=0.65$, unpaired two-tailed Student's *t* test). At 8 m, however, astrocytic volumes depended on the proximity to amyloid deposits. To assess whether proximity to amyloid plaques would differentially affect the volume of astrocytes in 8 m Tg mice, we calculated cellular volumes of GFAP immunoreactivity in two cell populations discriminated according to their distance to at least one amyloid plaque in the CA1 region of Tg mice. Fifty micrometers was set as the maximal distance between an astrocyte and at least one amyloid deposit that would grant inclusion of this astrocyte in the "plaque-associated" group (Figs. 4C and D). When analyzing astrocytes from Tg and NTg mice at 8 m, plaque-associated astrocytes displayed an increased volume in contrast with control astrocytes ($p<0.001$; two-way ANOVA, Bonferroni's *post hoc* test) whereas volume of non-plaque associated astrocytes was decreased ($p<0.05$ *vs.* NTg). The differential effect of the proximity to plaques was evident when comparing both cell populations in Tg mice: astrocytic volume was increased in areas surrounding extracellular amyloid deposits, in relation to that of astrocytes not associated to plaques ($p<0.001$ "proximity" effect, two-way ANOVA; Fig. 4F). To determine whether the observed changes were affected by EE, we compared astrocytic volume discriminating plaque-associated from non-plaque associated astrocytes. Exposure to EE did not significantly affect plaque-associated astrocyte volume ($p=0.13$). In contrast, the volume of non-plaque-associated astrocytes in Tg mice increased in response to EE ($p<0.01$ Tg EE *vs.* Tg in SC), reaching volumes that were similar to control astrocytes from NTg mice. In NTg mice we found no effect of the exposure to EE (Fig. 4F).

Altered astrocytic complexity in the hippocampus of APP mice. Effect of enriched environment

To determine the morphological complexity of GFAP+ cells, the degree of branching of processes was measured using Sholl analysis as previously described (Beauquis et al., 2010). Based on three-dimensional projections of confocal stack images through complete astrocytic extension, profiles of GFAP+ process were evaluated using image analysis software. The number of intersections for each concentric circle was calculated (Fig. 5). Processes of GFAP+ cells in 5 m Tg mice showed higher complexity than those of NTg animals ($p<0.0001$, genotype effect, two-way RM ANOVA). In 8 m animals, the complexity of processes of astrocytes that was not associated to plaques was higher in Tg mice than in NTg mice, regardless of the housing condition ($p<0.05$ for SC and $p<0.0001$ for EE, two-way ANOVA, Bonferroni's *post hoc* test). However, animals that were housed in an enriched environment showed decreased ramification of astrocytic processes ($p<0.0001$, housing effect, two-way RM ANOVA; Fig. 5C). Consistent with these observations, a trend to decreased complexity in processes of GFAP+ cells that was associated with plaques in 8 m Tg mice was detected with EE, but this difference did not reach statistical significance ($p=0.07$ housing effect, two-way RM ANOVA; Fig. 5D).

Discussion

Our results provide evidence regarding the effect of cognitive, social and sensorial stimulation on amyloid levels and astrocyte morphology in an animal model of Alzheimer's disease. We determined brain levels of amyloid β peptides, the presence of amyloid deposits in the hippocampus and the number and morphology of GFAP+ astrocytes in PDAPP-J20 transgenic mice, overexpressing a human APP gene carrying the Swedish and Indiana familial AD mutations at 5 m, before the onset of the overt amyloid brain pathology, and at 8 m when the presence of amyloid plaques has been previously described (Galvan et al., 2006). Exposure of PDAPP mice to EE for 3 months, overlapping the early progression of neuropathology in this mouse model, modulates the levels of Aβ 1–40 and 1–42 peptides in the brain and the morphology of glial cells in the hippocampus.

Exposure to EE lowered Aβ levels to levels comparable to those present in 5 m mice. The number and size of amyloid plaques in the hippocampus, however, did not change significantly after EE though a tendency towards a reduction was noted, suggesting that brain levels of Aβ

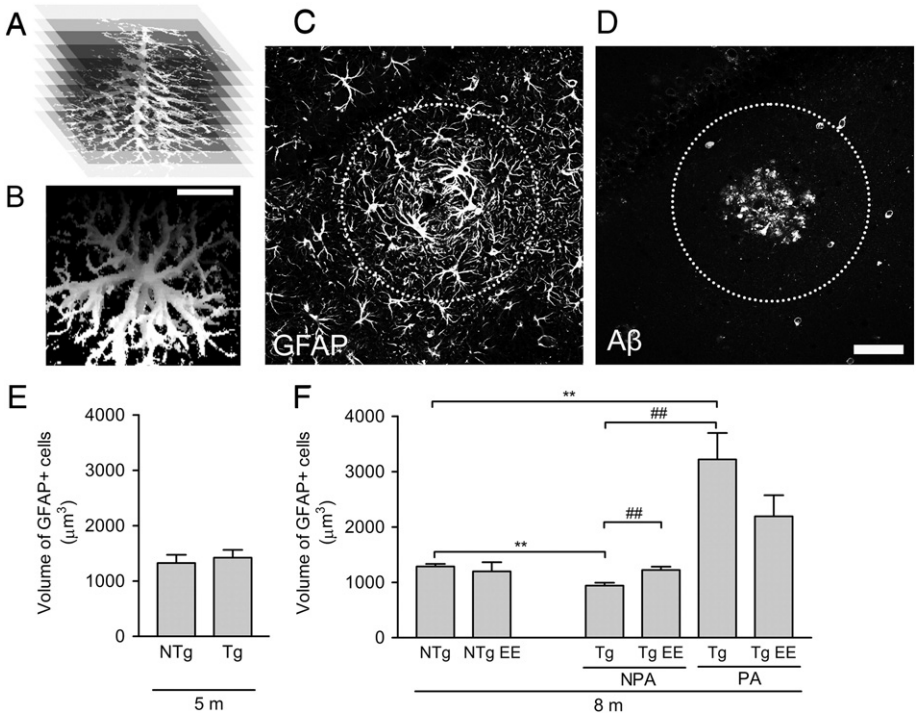

Fig. 4. Analysis of the volume of GFAP+ astrocytes in CA1 region. Panels A and B illustrate the reconstruction of GFAP+ astrocytes from serial confocal planes across each cell. Scale bar in panel B represents 20 μm. In panels C and D both channels of averaged confocal images are split to show GFAP cells in the vicinity of an amyloid plaque in stratum radiatum of hippocampus. The dotted-lined circle represents the criteria to separate cells associated to plaques (inside) from non-plaque-associated cells (outside). The perimeter is located at 50 μm from the border of the plaque. Scale bar in panel D represents 50 μm. At 5 months (5 m; panel E), no differences were found regarding the volume of GFAP+ astrocytes between both groups. At 8 months however (8 m; panel F), astrocytic volumes varied according to the distance to amyloid plaques. Plaque-associated astrocytes (PA) showed an increased volume compared with non-plaque associated cells (NPA; ##$p<0.01$ *vs.* Tg NPA and **$p<0.01$ *vs.* NTg; two-way ANOVA, Bonferroni's *post hoc* test; panel F). Non-plaque-associated astrocytes from Tg mice in SC displayed a decreased volume when compared with NTg (**$p<0.01$ *vs.* NTg 8 m) and the exposure of Tg mice to EE increased this parameter to control levels (##$p<0.01$ *vs.* Tg NPA).

peptides could correlate with hippocampal amyloid load and that a modulation of plaque deposition might be achieved with this strategy, as previously reported (Verret et al., in press).

There is evidence for the toxicity of Aβ peptides concerning synaptic alterations, abnormal tau phosphorylation, glial activation and neuronal loss (Tomiyama et al., 2010; Klein et al., 2001). Amyloid β peptides could be implicated in the cognitive and synaptic dysfunction present at early stages of AD (Lue et al., 1999). Available data indicates that the beneficial effects of EE on cognition could be associated with effects on the evolution of amyloid pathology, though conflicting results have been reported on animal modeling AD. This controversy might be related to differences in the models used. Not only does each model portray different aspects of the disease and its progression, but there are also variations related to the protocol of enrichment employed. For instance, Lazarov et al. reported decreased Aβ deposition together with diminished levels of soluble peptides and high Aβ degrading protease activity in APPsw × PS1ΔE9 mice after 5 months of EE that included physical activity. Increased spontaneous running time correlated with less plaque deposition in the brain (Lazarov et al., 2005). Herring et al. also reported fewer Aβ deposits in hippocampus of TgCRND8 mice after 4 m of EE that included exercise, without changes in Aβ peptides (Herring et al., 2008). In contrast, Jankowsky et al. reported increased plaque deposition and levels of Aβ after EE in APP/PS1 transgenic mice (Jankowsky et al., 2003; Jankowsky et al., 2003), whereas other group reported no changes in amyloid β load in parietal cortex and hippocampus, but improved cognitive function in APPsw transgenic mice (Arendash et al., 2004). In a recent study it was reported that exposure to EE induces a decreased amyloid plaque load in hippocampus and forebrain of Tg2576 mice only when started at an early age (3 months) and not at advanced ages (Verret et al., in press) suggesting that an early intervention is necessary to prevent the progression of amyloid pathology. Multiple mechanisms can be involved in lowering Aβ levels and thus improving cognitive and neuronal outcomes as a result of EE. Decreased amyloidogenic processing of APP has been described in response to EE in a model of ischemia-induced amyloidogenesis (Briones et al., 2009). In the same model and also in APP-PS1 transgenic mice an increase in the levels of Aβ degrading enzymes like insulin-degrading enzyme and neprilysin was reported after EE (Briones et al., 2009; Lazarov et al., 2005). Another pathway that could be implicated in Aβ clearance is the transport through the blood–brain barrier. Molecules implicated in the movement across the brain are known to be regulated by EE. Using TgCRND8 APP transgenic mice, Herring et al. found that EE, through increased neuronal activity, upregulates LRP1 and its ligands, ApoE and A2M, and downregulates RAGE thus facilitating the clearance of Aβ from the brain (Herring et al., 2008). Also, perivascular astrocytes could contribute to the clearance of ApoE-associated Aβ as demonstrated by Rolyan et al. (2011), probably participating in the modulation of AD pathogenesis. As it was lately emphasized, glial endocytic activity could play a relevant role (Mulder et al., 2012; Thal, 2012). In consonance with Rodriguez et al. in the 3xTg mice (Rodriguez et al., 2009), we observed specific cytoplasmic Aβ immunoreactivity in GFAP+ astrocytes surrounding plaques in PDAPP mice (colocalization study illustrated in Supplementary Fig. 1). Available data also indicates that activated phagocytic microglia could contribute to Aβ peptides endocytosis (Wyss-Coray et al., 2001). Also, mechanisms associated with the autophagic process can be mediating this effect. Galvan et al. reported a considerable diminution of Aβ 1–42 levels subsequent to mTOR pathway inhibition by rapamycin in PDAPP-J20 mice (Spilman et al., 2010).

In the present work, at 5 m, an early temporal point of the disease in the studied animal model, we found a reduction in number of GFAP+ astrocytes in the hippocampus. The observed decrease could represent an early event in the progression of AD-like pathology; however, this reduction was not seen at 8 m, suggesting that the astrocytic population decreases early during the pathogenesis of AD-like deficits in PDAPP

mice but some compensating mechanism is activated later on. The early and transient reduction in cell number could be due to decreased gliogenesis and/or to increased cell death in PDAPP mice. At 8 months, when amyloid plaques are present in the hippocampus, reactive astrogliosis could implicate proliferation of GFAP+ astrocytes as it has been described previously (Vijayan et al., 1991; Beach et al., 1989) and thus compensate the baseline decreased cell number. In PDAPP-J20 Tg mice, a 4.5 fold increase in the number of GFAP+ astrocytes has been described in the hippocampus at 12 months of age (Galvan et al., 2006). Also, in human postmortem brain samples, it has been reported that astroglial proliferation is present in the presenile hippocampus (Boekhoorn et al., 2006). The 8-month age point studied in the present work represents an intermediate stage in the progression of the disease. Although GFAP+ cells represent more than 90% of total hippocampal astrocytes (Jinno, 2011), thus constituting a reliable marker of astroglia, the representation of other astroglial phenotypes could be altered in a pathological condition such as AD-like pathogenesis. Studies and preliminary data including other markers show us that a high proportion of GFAP positive astrocytes are also positive for s100B (Supplementary Fig. 2; Jinno, 2011). The decreased number of GFAP+ astrocytes seen at 5 months could be due to a shift in the glial marker expressed and not to a net decrease in the total number of astrocytes. Different cell maturation dynamics rather than absolute cell number decrease could underlie the difference in GFAP+ astrocyte number (Raponi et al., 2007).

A reduction of GFAP+ cell volume in astrocytes distant from amyloid deposits was found in Tg mice at 8 months. In contrast, astroglia in close association with amyloid plaques displayed an augmented reactivity characterized by a 3-fold increase in the cellular volume in comparison with control astrocytes. Astrocyte pathology occurs in association with AD and other CNS pathologies and a large number of studies have been reported on this topic (Kuchibhotla et al., 2009; Nagele et al., 2004; Parpura and Verkhratsky, 2012). How changes in astroglial phenotype morphology are related to AD pathogenesis, however, is still incompletely understood. Interestingly, Rodriguez et al. reported concomitant glial atrophy and astrogliosis in 3xTg-AD mice, a mouse model harboring mutations in APP, PS1 and tau genes (Olabarria et al., 2010). In that study, GFAP+ astrocytes showed a dual behavior depending on the distance to Aβ plaques: astrogliosis, described as an increase in the surface and volume of GFAP+ cells, was found in the proximity of amyloid plaques whereas astrocytes located away from Aβ deposits showed atrophic changes, in a similar fashion to that found in the present work. These results and ours, showing glial abnormalities linked to AD pathology and shared by 3xTg-AD and PDAPP transgenic mice, could suggest an association of astrocytic alterations to the amyloidogenic pathway more than to tau pathology.

We found an increased branching of GFAP+ astroglial processes in the hippocampus of Tg mice both at 5 and 8 months. However, this change was present even in astrocytes located far from Aβ plaques that also showed decreased GFAP+ cell volume. This apparently paradoxical result could be originated by a differential regulation of astroglial branching and volume. Alterations in the glial cytoskeleton could be a secondary reaction to premature neuronal changes, as synaptic perturbations, that occur before plaque formation (Scheff et al., 2007). In an electron microscopy study by Geinisman et al., an increase in the ramification and/or elongation of astroglial processes was found in the hippocampus of senescent rats, potentially constituting a compensating mechanism for dendritic loss (Geinisman et al., 1978). Decreased astrocytic volume could be secondary to impaired synaptic connectivity and altered transcription of cytoskeleton-related genes,

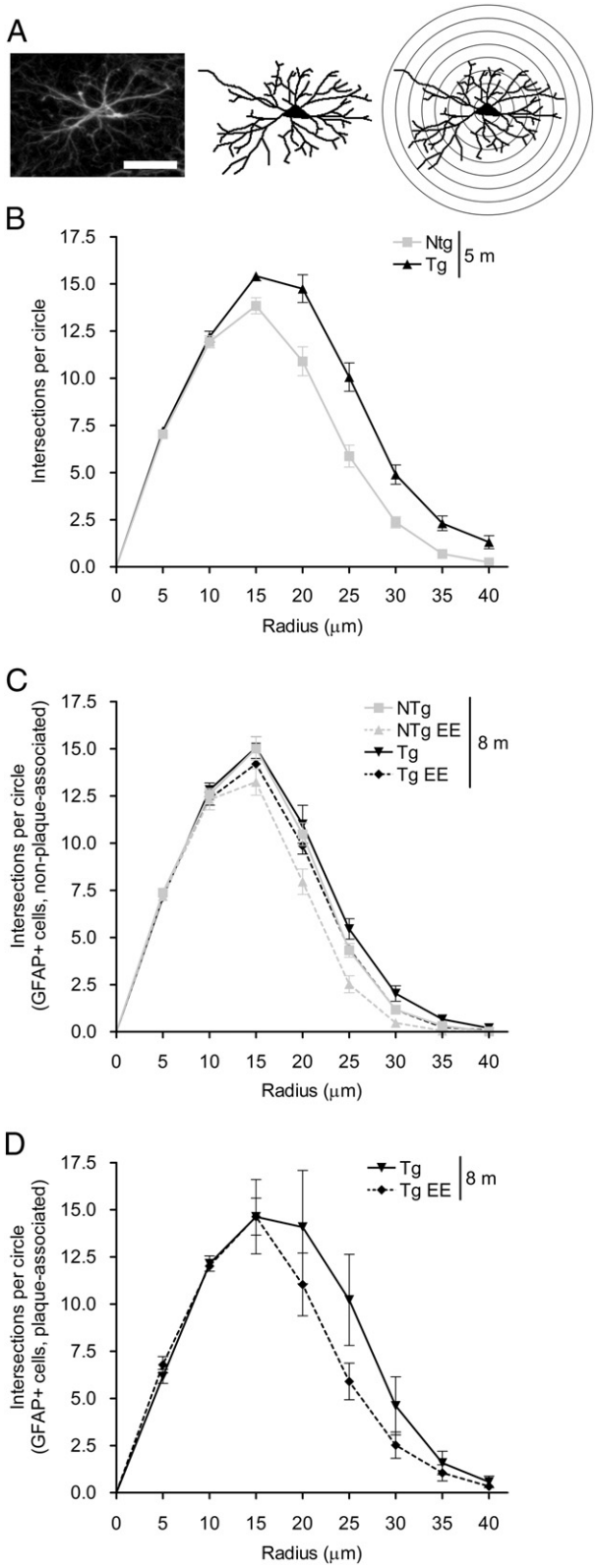

Fig. 5. Sholl analysis of GFAP+ astrocytes in CA1 region. Panel A shows an averaged image of multiple confocal planes across a GFAP+ astrocyte (left), the traced profile of the same cell (middle) and a figure to illustrate the position of the concentric circles used for Sholl analysis (right). Scale bar in panel A represents 20 μm. At 5 months (5 m; panel B), Tg mice presented astrocytes with an increased ramification compared with NTg ($p<0.0001$; 2-way RM ANOVA). When evaluating non-plaque-associated astrocytes in 8-month-old (8 m) Tg mice (panel C), cell morphology was more complex than in NTg regardless of the housing condition ($p<0.05$ for SC and $p<0.0001$ for EE). Housing in the enriched environment determined a decrease in the astrocytic ramification in both genotypes ($p<0.0001$). In the analysis of plaque-associated astrocytes, we did not find significant differences between Tg in SC and Tg in EE though a tendency towards a decrease with EE was noted (panel D).

phenomena described in the context of AD (Scheff et al., 2007; Simpson et al., 2011).

In our study, the exposure to EE prevented astroglial morphological and volume changes associated with the progression of AD-like pathogenesis in PDAPP mice, resulting in parameters similar to those of non-transgenic animals. This fact could be a result of the significant decreases in Aβ levels following EE (Lazarov et al., 2005; Herring et al., 2008; Valero et al., 2011). Previous reports also showed morphological changes in glia as a result of EE in young and healthy mice (Viola et al., 2009). Astrocytes can modify their morphology in response to neurotrophins acting through TrkB T1 receptor (Ohira et al., 2007) and these morphological alterations might be essential for synaptic plasticity and maintenance (Benediktsson et al., 2005). Also, receptors for different types of neurotransmitters were found in astrocytes, suggesting a possible pathway through which they can respond to neuronal activity (Murphy and Pearce, 1987). Also, the effects of EE preventing astroglial morphological alterations could be mediated through a mitigation of the inflammatory response. Williamson et al. showed an attenuation of the glial pro-inflammatory profile in hippocampi from rats exposed to a rich environment (Williamson et al., 2012). Neuroinflammatory changes have been identified as a key component of the disease, together with amyloid β deposition and neurofibrillary tangles. Based on existing data, this reactive astrocytic population found surrounding plaques could be able to secrete, in concert with microglia, a wide variety of pro-inflammatory molecules (Krause and Muller, 2010).

Multiple protocols of EE have been reported and the main difference can be found regarding physical exercise, with some of them including a device for physical activity (e.g. running wheel) and others not. In the present work and in a previous study (Beauquis et al., 2010), we did not include physical activity in order to isolate the effect of 'pure' EE. In animal models of diabetes mellitus and Parkinson's disease, exposure to treadmill exercise prevents the decrease of hippocampal GFAP optical density associated with the pathology (de Senna et al., 2011; Dutra et al., 2012). Also, it has been reported that running, but not enrichment, strongly induced net astrogliogenesis in adult mice (Steiner et al., 2004). Effects of physical activity on neuronal plasticity could be different from those of EE and may not always implicate the same pathways (Olson et al., 2006).

Our results demonstrate that glial changes in the context of AD-like progression can be prevented by the exposure to EE and thus contribute to our understanding of the high complexity of the neuro-glial plasticity in response to environmental stimuli. The observed rescue of GFAP+ astroglial volume and process complexity in 8 m PDAPP transgenic mice suggests that EE induced increases in volume of the soma while decreasing process complexity. Thus, our results suggest that glia in PDAPP mice can respond to environmental stimuli adopting a morphology similar to that found in control mice. This phenomenon could be associated with a recovery in their neuroprotective function, regarding energy metabolism, recycling of neurotransmitters and antioxidant capacity (Li et al., 1997; Masliah et al., 1996; Fuller et al., 2010; Newman et al., 2007; Steele and Robinson, 2012). The effect of EE promoting neuroprotection in AD Tg mice was demonstrated in multiple studies (Valero et al., 2011; Arendash et al., 2004; Costa et al., 2007; Jankowsky et al., 2005), and probably implicates simultaneous cellular and molecular responses that take place in a plastic brain area as the hippocampus. Our results show that exposure to environmental stimuli can also induce glial changes that could be translated, as mentioned, into an improved neuronal metabolic support and clearance of proteins, including Aβ, from extracellular space, among other effects. The possibility to enhance or potentiate endogenous protective pathways that allow the organism to resist the neurodegenerative process in a more successful manner is strongly attractive. The fact that this strategy involves modulation of glial cells, that seem to be affected early in AD, and a potential restoration of function in astrocytes, that constitute the predominant cell type in the brain, adds a remarkably amplifying effect. Another relevant point of this study is the nature of the proposed strategy, employing a nonpharmacological approach promoting and reinforcing the cognitive reserve as an endogenous system of protection. In conclusion, the modulation of glial functionality through environmental intervention may constitute an attractive and relatively simple target for therapy.

Supplementary data to this article can be found online at http://dx.doi.org/10.1016/j.expneurol.2012.09.009.

Conflict of interest

The authors declare that no competing interests exist.

Acknowledgments

The authors thank Pablo Do Campo for his assistance with confocal microscopy and the personnel of the animal facility at the Instituto de Biología y Medicina Experimental (IBYME) for their help with animal care. JB is a recipient of a post-doctoral fellowship from the Consejo Nacional de Investigaciones Científicas y Técnicas of Argentina (CONICET). FS is a career investigator from CONICET. This work was supported by a grant to FS from the Agencia Nacional de Promoción de Ciencia y Tecnología of Argentina (PICT 2011, #1012).

References

Abramoff, M.D., Magelhaes, P.J., Ram, S.J., 2004. Image processing with ImageJ. Biophotonics Int. 11, 36–42.
Akiyama, H., Mori, H., Saido, T., Kondo, H., Ikeda, K., McGeer, P.L., 1999. Occurrence of the diffuse amyloid beta-protein (Abeta) deposits with numerous Abeta-containing glial cells in the cerebral cortex of patients with Alzheimer's disease. Glia 25, 324–331.
Arendash, G.W., Garcia, M.F., Costa, D.A., Cracchiolo, J.R., Wefes, I.M., Potter, H., 2004. Environmental enrichment improves cognition in aged Alzheimer's transgenic mice despite stable beta-amyloid deposition. Neuroreport 15, 1751–1754.
Arranz, L., De Castro, N.M., Baeza, I., Gimenez-Llort, L., la FM, De, 2011. Effect of environmental enrichment on the immunoendocrine aging of male and female triple-transgenic 3xTg-AD mice for Alzheimer's disease. J. Alzheimers Dis. 25, 727–737.
Beach, T.G., Walker, R., McGeer, E.G., 1989. Patterns of gliosis in Alzheimer's disease and aging cerebrum. Glia 2, 420–436.
Beauquis, J., Roig, P., De Nicola, A.F., Saravia, F., 2010. Short-term environmental enrichment enhances adult neurogenesis, vascular network and dendritic complexity in the hippocampus of type 1 diabetic mice. PLoS One 5, e13993.
Benediktsson, A.M., Schachtele, S.J., Green, S.H., Dailey, M.E., 2005. Ballistic labeling and dynamic imaging of astrocytes in organotypic hippocampal slice cultures. J. Neurosci. Methods 141, 41–53.
Bindu, B., Alladi, P.A., Mansooralikhan, B.M., Srikumar, B.N., Raju, T.R., Kutty, B.M., 2007. Short-term exposure to an enriched environment enhances dendritic branching but not brain-derived neurotrophic factor expression in the hippocampus of rats with ventral subicular lesions. Neuroscience 144, 412–423.
Boekhoorn, K., Joels, M., Lucassen, P.J., 2006. Increased proliferation reflects glial and vascular-associated changes, but not neurogenesis in the presenile Alzheimer hippocampus. Neurobiol. Dis. 24, 1–14.
Braak, H., Braak, E., 1998. Evolution of neuronal changes in the course of Alzheimer's disease. J. Neural Transm. Suppl. 53, 127–140.
Briones, T.L., Rogozinska, M., Woods, J., 2009. Environmental experience modulates ischemia-induced amyloidogenesis and enhances functional recovery. J. Neurotrauma 26, 613–625.
Carter, S.F., Scholl, M., Almkvist, O., Wall, A., Engler, H., Langstrom, B., Nordberg, A., 2012. Evidence for astrocytosis in prodromal Alzheimer disease provided by 11C-deuterium-L-deprenyl: a multitracer PET paradigm combining 11C-Pittsburgh compound B and 18F-FDG. J. Nucl. Med. 53, 37–46.
Costa, D.A., Cracchiolo, J.R., Bachstetter, A.D., Hughes, T.F., Bales, K.R., Paul, S.M., Mervis, R.F., et al., 2007. Enrichment improves cognition in AD mice by amyloid-related and unrelated mechanisms. Neurobiol. Aging 28, 831–844.
Cotel, M.C., Jawhar, S., Christensen, D.Z., Bayer, T.A., Wirths, O., 2012. Environmental enrichment fails to rescue working memory deficits, neuron loss, and neurogenesis in APP/PS1KI mice. Neurobiol. Aging 33, 96–107.
de Senna, P.N., Ilha, J., Baptista, P.P., do Nascimento, P.S., Leite, M.C., Paim, M.F., Goncalves, C.A., et al., 2011. Effects of physical exercise on spatial memory and astroglial alterations in the hippocampus of diabetic rats. Metab. Brain Dis. 26, 269–279.
Dickson, D.W., 1997. Neuropathological diagnosis of Alzheimer's disease: a perspective from longitudinal clinicopathological studies. Neurobiol. Aging 18, S21–S26.
Dutra, M.F., Jaeger, M., Ilha, J., Kalil-Gaspar, P.I., Marcuzzo, S., Achaval, M., 2012. Exercise improves motor deficits and alters striatal GFAP expression in a 6-OHDA-induced rat model of Parkinson's disease. Neurol. Sci. 33 (5), 1137–1144.

Fuller, S., Steele, M., Munch, G., 2010. Activated astroglia during chronic inflammation in Alzheimer's disease—do they neglect their neurosupportive roles? Mutat. Res. 690, 40–49.
Galvan, V., Gorostiza, O.F., Banwait, S., Ataie, M., Logvinova, A.V., Sitaraman, S., Carlson, E., et al., 2006. Reversal of Alzheimer's-like pathology and behavior in human APP transgenic mice by mutation of Asp664. Proc. Natl. Acad. Sci. U. S. A. 103, 7130–7135.
Geinisman, Y., Bondareff, W., Dodge, J.T., 1978. Hypertrophy of astroglial processes in the dentate gyrus of the senescent rat. Am. J. Anat. 153, 537–543.
Giaume, C., Kirchhoff, F., Matute, C., Reichenbach, A., Verkhratsky, A., 2007. Glia: the fulcrum of brain diseases. Cell Death Differ. 14, 1324–1335.
Gundersen, H.J., Bagger, P., Bendtsen, T.F., Evans, S.M., Korbo, L., Marcussen, N., Moller, A., et al., 1988. The new stereological tools: disector, fractionator, nucleator and point sampled intercepts and their use in pathological research and diagnosis. APMIS 96, 857–881.
Hebb, D.O., 1947. The effects of early experience on problem-solving at maturity. Am. Psychol. 2, 306–307.
Heneka, M.T., Rodriguez, J.J., Verkhratsky, A., 2010. Neuroglia in neurodegeneration. Brain Res. Rev. 63, 189–211.
Herring, A., Yasin, H., Ambree, O., Sachser, N., Paulus, W., Keyvani, K., 2008. Environmental enrichment counteracts Alzheimer's neurovascular dysfunction in TgCRND8 mice. Brain Pathol. 18, 32–39.
Hou, L., Liu, Y., Wang, X., Ma, H., He, J., Zhang, Y., Yu, C., et al., 2011. The effects of amyloid-beta42 oligomer on the proliferation and activation of astrocytes *in vitro*. In Vitro Cell. Dev. Biol. Anim. 47, 573–580.
Hsia, A.Y., Masliah, E., McConlogue, L., Yu, G.Q., Tatsuno, G., Hu, K., Kholodenko, D., et al., 1999. Plaque-independent disruption of neural circuits in Alzheimer's disease mouse models. Proc. Natl. Acad. Sci. U. S. A. 96, 3228–3233.
Jankowsky, J.L., Xu, G., Fromholt, D., Gonzales, V., Borchelt, D.R., 2003. Environmental enrichment exacerbates amyloid plaque formation in a transgenic mouse model of Alzheimer disease. J. Neuropathol. Exp. Neurol. 62, 1220–1227.
Jankowsky, J.L., Melnikova, T., Fadale, D.J., Xu, G.M., Slunt, H.H., Gonzales, V., Younkin, L.H., et al., 2005. Environmental enrichment mitigates cognitive deficits in a mouse model of Alzheimer's disease. J. Neurosci. 25, 5217–5224.
Jinno, S., 2011. Regional and laminar differences in antigen profiles and spatial distributions of astrocytes in the mouse hippocampus, with reference to aging. Neuroscience 180, 41–52.
Kempermann, G., Kuhn, H., Gage, F., 1997. More hippocampal neurons in adult mice living in an enriched environment. Nature 386, 493–495.
Kempermann, G., Kuhn, H.G., Gage, F.H., 1998. Experience-induced neurogenesis in the senescent dentate gyrus. J. Neurosci. 18, 3206–3212.
Klein, W.L., Krafft, G.A., Finch, C.E., 2001. Targeting small Abeta oligomers: the solution to an Alzheimer's disease conundrum? Trends Neurosci. 24, 219–224.
Krause, D.L., Muller, N., 2010. Neuroinflammation, microglia and implications for anti-inflammatory treatment in Alzheimer's disease. Int. J. Alzheimers Dis. pii:732806.
Krech, D., Rosenzweig, M.R., Bennett, E.L., 1962. Relations between chemistry and problem-solving among rats raised in enriched and impoverished environments. J. Comp. Physiol. Psychol. 55, 801–807.
Kuchibhotla, K.V., Lattarulo, C.R., Hyman, B.T., Bacskai, B.J., 2009. Synchronous hyperactivity and intercellular calcium waves in astrocytes in Alzheimer mice. Science 323, 1211–1215.
Lazarov, O., Robinson, J., Tang, Y.P., Hairston, I.S., Korade-Mirnics, Z., Lee, V.M., Hersh, L.B., et al., 2005. Environmental enrichment reduces Abeta levels and amyloid deposition in transgenic mice. Cell 120, 701–713.
Li, S., Mallory, M., Alford, M., Tanaka, S., Masliah, E., 1997. Glutamate transporter alterations in Alzheimer disease are possibly associated with abnormal APP expression. J. Neuropathol. Exp. Neurol. 56, 901–911.
Lue, L.F., Kuo, Y.M., Roher, A.E., Brachova, L., Shen, Y., Sue, L., Beach, T., et al., 1999. Soluble amyloid beta peptide concentration as a predictor of synaptic change in Alzheimer's disease. Am. J. Pathol. 155, 853–862.
Masliah, E., Alford, M., DeTeresa, R., Mallory, M., Hansen, L., 1996. Deficient glutamate transport is associated with neurodegeneration in Alzheimer's disease. Ann. Neurol. 40, 759–766.
Massoud, F., Leger, G.C., 2011. Pharmacological treatment of Alzheimer disease. Can. J. Psychiatry 56, 579–588.
Mattson, M.P., 2004. Pathways towards and away from Alzheimer's disease. Nature 430, 631–639.
Mayeux, R., 2010. Clinical practice. Early Alzheimer's disease. N. Engl. J. Med. 362, 2194–2201.
Mirochnic, S., Wolf, S., Staufenbiel, M., Kempermann, G., 2009. Age effects on the regulation of adult hippocampal neurogenesis by physical activity and environmental enrichment in the APP23 mouse model of Alzheimer disease. Hippocampus 19, 1008–1018.
Mucke, L., Masliah, E., Yu, G.Q., Mallory, M., Rockenstein, E.M., Tatsuno, G., Hu, K., et al., 2000. High-level neuronal expression of abeta 1–42 in wild-type human amyloid protein precursor transgenic mice: synaptotoxicity without plaque formation. J. Neurosci. 20, 4050–4058.
Mulder, S.D., Veerhuis, R., Blankenstein, M.A., Nielsen, H.M., 2012. The effect of amyloid associated proteins on the expression of genes involved in amyloid-beta clearance by adult human astrocytes. Exp. Neurol. 233, 373–379.
Murphy, S., Pearce, B., 1987. Functional receptors for neurotransmitters on astroglial cells. Neuroscience 22, 381–394.
Murray, A.D., Staff, R.T., McNeil, C.J., Salarirad, S., Ahearn, T.S., Mustafa, N., Whalley, L.J., 2011. The balance between cognitive reserve and brain imaging biomarkers of cerebrovascular and Alzheimer's diseases. Brain 134, 3687–3696.
Nagele, R.G., Wegiel, J., Venkataraman, V., Imaki, H., Wang, K.C., Wegiel, J., 2004. Contribution of glial cells to the development of amyloid plaques in Alzheimer's disease. Neurobiol. Aging 25, 663–674.
Nedergaard, M., Dirnagl, U., 2005. Role of glial cells in cerebral ischemia. Glia 50, 281–286.
Newman, S.F., Sultana, R., Perluigi, M., Coccia, R., Cai, J., Pierce, W.M., Klein, J.B., et al., 2007. An increase in S-glutathionylated proteins in the Alzheimer's disease inferior parietal lobule, a proteomics approach. J. Neurosci. Res. 85, 1506–1514.
Nithianantharajah, J., Hannan, A.J., 2006. Enriched environments, experience-dependent plasticity and disorders of the nervous system. Nat. Rev. Neurosci. 7, 697–709.
Ohira, K., Funatsu, N., Homma, K.J., Sahara, Y., Hayashi, M., Kaneko, T., Nakamura, S., 2007. Truncated TrkB-T1 regulates the morphology of neocortical layer I astrocytes in adult rat brain slices. Eur. J. Neurosci. 25, 406–416.
Olabarria, M., Noristani, H.N., Verkhratsky, A., Rodriguez, J.J., 2010. Concomitant astroglial atrophy and astrogliosis in a triple transgenic animal model of Alzheimer's disease. Glia 58, 831–838.
Olson, A.K., Eadie, B.D., Ernst, C., Christie, B.R., 2006. Environmental enrichment and voluntary exercise massively increase neurogenesis in the adult hippocampus *via* dissociable pathways. Hippocampus 16, 250–260.
Parpura, V., Verkhratsky, A., 2012. Neuroglia at the crossroads of homeostasis, metabolism and signaling: evolution of the concept. ASN Neuro 4 (4), 201–205.
Pekny, M., Nilsson, M., 2005. Astrocyte activation and reactive gliosis. Glia 50, 427–434.
Querfurth, H.W., LaFerla, F.M., 2010. Alzheimer's disease. N. Engl. J. Med. 362, 329–344.
Raponi, E., Agenes, F., Delphin, C., Assard, N., Baudier, J., Legraverend, C., Deloulme, J.C., 2007. S100B expression defines a state in which GFAP-expressing cells lose their neural stem cell potential and acquire a more mature developmental stage. Glia 55, 165–177.
Roberson, E.D., Scearce-Levie, K., Palop, J.J., Yan, F., Cheng, I.H., Wu, T., Gerstein, H., et al., 2007. Reducing endogenous tau ameliorates amyloid beta-induced deficits in an Alzheimer's disease mouse model. Science 316, 750–754.
Rodriguez, J.J., Olabarria, M., Chvatal, A., Verkhratsky, A., 2009. Astroglia in dementia and Alzheimer's disease. Cell Death Differ. 16, 378–385.
Rolyan, H., Feike, A.C., Upadhaya, A.R., Waha, A., Van Dooren, T., Haass, C., Birkenmeier, G., et al., 2011. Amyloid-beta protein modulates the perivascular clearance of neuronal apolipoprotein E in mouse models of Alzheimer's disease. J. Neural Transm. 118, 699–712.
Scheff, S.W., Price, D.A., Schmitt, F.A., DeKosky, S.T., Mufson, E.J., 2007. Synaptic alterations in CA1 in mild Alzheimer disease and mild cognitive impairment. Neurology 68, 1501–1508.
Selkoe, D.J., 2000. Toward a comprehensive theory for Alzheimer's disease. Hypothesis: Alzheimer's disease is caused by the cerebral accumulation and cytotoxicity of amyloid beta-protein. Ann. N. Y. Acad. Sci. 924, 17–25.
Sholl, D.A., 1953. Dendritic organization in the neurons of the visual and motor cortices of the cat. J. Anat. 87, 387–406.
Simpson, J.E., Ince, P.G., Shaw, P.J., Heath, P.R., Raman, R., Garwood, C.J., Gelsthorpe, C., et al., 2011. Microarray analysis of the astrocyte transcriptome in the aging brain: relationship to Alzheimer's pathology and APOE genotype. Neurobiol. Aging 32, 1795–1807.
Sirevaag, A.M., Greenough, W.T., 1991. Plasticity of GFAP-immunoreactive astrocyte size and number in visual cortex of rats reared in complex environments. Brain Res. 540, 273–278.
Spilman, P., Podlutskaya, N., Hart, M.J., Debnath, J., Gorostiza, O., Bredesen, D., Richardson, A., et al., 2010. Inhibition of mTOR by rapamycin abolishes cognitive deficits and reduces amyloid-beta levels in a mouse model of Alzheimer's disease. PLoS One 5, e9979.
Steele, M.L., Robinson, S.R., 2012. Reactive astrocytes give neurons less support: implications for Alzheimer's disease. Neurobiol. Aging 33 (2), 423.e1-13.
Steiner, B., Kronenberg, G., Jessberger, S., Brandt, M.D., Reuter, K., Kempermann, G., 2004. Differential regulation of gliogenesis in the context of adult hippocampal neurogenesis in mice. Glia 46, 41–52.
Thal, D.R., 2012. The role of astrocytes in amyloid beta-protein toxicity and clearance. Exp. Neurol. 236, 1–5.
Thal, D.R., Schultz, C., Dehghani, F., Yamaguchi, H., Braak, H., Braak, E., 2000. Amyloid beta-protein (Abeta)-containing astrocytes are located preferentially near N-terminal-truncated Abeta deposits in the human entorhinal cortex. Acta Neuropathol. 100, 608–617.
Tian, G.F., Azmi, H., Takano, T., Xu, Q., Peng, W., Lin, J., Oberheim, N., et al., 2005. An astrocytic basis of epilepsy. Nat. Med. 11, 973–981.
Tomiyama, T., Matsuyama, S., Iso, H., Umeda, T., Takuma, H., Ohnishi, K., Ishibashi, K., et al., 2010. A mouse model of amyloid beta oligomers: their contribution to synaptic alteration, abnormal tau phosphorylation, glial activation, and neuronal loss in vivo. J. Neurosci. 30, 4845–4856.
Valero, J., Espana, J., Parra-Damas, A., Martin, E., Rodriguez-Alvarez, J., Saura, C.A., 2011. Short-term environmental enrichment rescues adult neurogenesis and memory deficits in APP(Sw, Ind) transgenic mice. PLoS One 6, e16832.
van Praag, H., Kempermann, G., Gage, F.H., 2000. Neural consequences of environmental enrichment. Nat. Rev. Neurosci. 1, 191–198.
Verret, L., Krezymon, A., Halley, H., Trouche, S., Zerwas, M., Lazouret, M., Lassalle, J.M., et al., in press. Transient enriched housing before amyloidosis onset sustains cogni-tive improvement in Tg2576 mice. Neurobiol Aging. http://dx.doi.org/10.1016/j.neurobiolaging.2012.05.013. (Electronic publication ahead of print).
Vijayan, V.K., Geddes, J.W., Anderson, K.J., Chang-Chui, H., Ellis, W.G., Cotman, C.W., 1991. Astrocyte hypertrophy in the Alzheimer's disease hippocampal formation. Exp. Neurol. 112, 72–78.
Viola, G.G., Rodrigues, L., Americo, J.C., Hansel, G., Vargas, R.S., Biasibetti, R., Swarowsky, A., et al., 2009. Morphological changes in hippocampal astrocytes induced by environmental enrichment in mice. Brain Res. 1274, 47–54.
Webster, B., Hansen, L., Adame, A., Crews, L., Torrance, M., Thal, L., Masliah, E., 2006. Astroglial activation of extracellular-regulated kinase in early stages of Alzheimer disease. J. Neuropathol. Exp. Neurol. 65, 142–151.

Wilcock, D.M., Gordon, M.N., Morgan, D., 2006. Quantification of cerebral amyloid angiopathy and parenchymal amyloid plaques with Congo red histochemical stain. Nat. Protoc. 1, 1591–1595.
Williamson, L.L., Chao, A., Bilbo, S.D., 2012. Environmental enrichment alters glial antigen expression and neuroimmune function in the adult rat hippocampus. Brain Behav. Immun. 26, 500–510.
Wyss-Coray, T., Lin, C., Yan, F., Yu, G.Q., Rohde, M., McConlogue, L., Masliah, E., et al., 2001. TGF-beta1 promotes microglial amyloid-beta clearance and reduces plaque burden in transgenic mice. Nat. Med. 7, 612–618.
Yeh, C.Y., Vadhwana, B., Verkhratsky, A., Rodriguez, J.J., 2011. Early astrocytic atrophy in the entorhinal cortex of a triple transgenic animal model of Alzheimer's disease. ASN Neuro 3, 271–279.